

Tuning low-energy scales in YbRh_2Si_2 by non-isoelectronic substitution and pressure

M.-H. Schubert,¹ Y. Tokiwa,² S.-H. Hübner,¹ M. Mchalwat,¹ E. Blumenröther,¹ H. S. Jeevan,¹ and P. Gegenwart²

¹*I. Physikalisches Institut, Georg-August-Universität Göttingen, D-37077 Göttingen, Germany*

²*Experimental Physics VI, Center for Electronic Correlations and Magnetism, University of Augsburg, 86159 Augsburg, Germany*



(Received 14 March 2019; revised manuscript received 23 May 2019; published 8 October 2019)

The heavy-fermion metal YbRh_2Si_2 realizes a field-induced quantum critical point with multiple vanishing energy scales $T_N(B)$ and $T^*(B)$. We investigate their change with partial non-isoelectronic substitutions, chemical and hydrostatic pressure. Low-temperature electrical resistivity, specific heat, and magnetic susceptibility of $\text{Yb}(\text{Rh}_{1-x}\text{T}_x)_2\text{Si}_2$ with $T = \text{Fe}$ or Ni for $x \leq 0.1$, magnetic fields $B \leq 0.3$ T (applied perpendicular to the c axis), and hydrostatic pressure $p \leq 1.5$ GPa are reported. The data allow us to disentangle the combined influences of hydrostatic and chemical pressure, as well as non-isoelectronic substitution. In contrast to Ni and Co substitution, which enhance magnetic order, Fe substitution acts oppositely. For $x = 0.1$, it also completely suppresses the T^* crossover and eliminates ferromagnetic fluctuations. The pressure, magnetic field, and temperature dependences of T^* are incompatible with its interpretation as Kondo breakdown signature.

DOI: [10.1103/PhysRevResearch.1.032004](https://doi.org/10.1103/PhysRevResearch.1.032004)

Quantum phase transitions are of central importance in correlated materials. Whether well-defined quasiparticles exist at a quantum critical point (QCP) is relevant for understanding cuprates and heavy-fermion metals [1,2]. The latter consist of lattices of certain f electrons and realize quantum criticality arising from two competing interactions: the indirect exchange coupling (RKKY interaction) between the f electrons, mediated by conduction electrons, and the Kondo screening acting on each f moment site. Since both interactions depend on the antiferromagnetic (AF) exchange J between f and conduction electrons, quantum criticality is realized by tuning J with pressure, chemical substitution, or magnetic field [3,4]. Several heavy-fermion metals have been studied near QCPs, revealing non-Fermi-liquid (NFL) behavior, as well as the occurrence of unconventional superconductivity [5].

Tetragonal YbRh_2Si_2 with very weak AF ordering at $T_N = 70$ mK is one of the best studied model systems for quantum criticality in heavy-fermion metals [6]. By application of a small critical magnetic field $B_c = 0.06$ T ($B \perp c$), it displays a QCP and paramagnetic Fermi liquid behavior occurs at $B > B_c$ [7]. Hydrostatic pressure [8] or chemical pressure [9], induced by few atomic percent (%) substitution of Rh by isoelectronic Co, stabilizes the AF ordering and enhances the critical field B_c . Vice versa, volume expansion induced by negative chemical pressure weakens the AF ordering and reduces B_c [2,9]. Close to the field-induced QCP a quasilinear temperature dependence of the electrical resistivity and divergences of the specific heat coefficient [7], magnetic susceptibility [10], and Grüneisen parameters [11,12] indicate NFL

properties that are incompatible with the theory of itinerant AF quantum criticality [13].

Measurements of the isothermal field dependence of the Hall coefficient, magnetoresistance, magnetostriction, magnetization, and entropy have revealed a crossover scale labeled $T^*(B)$ or $B^*(T)$ [14–16]. This crossover is independent from the boundary of the AF order $T_N(B)$ and the Fermi-liquid crossover in electrical resistivity, although it merges for undoped YbRh_2Si_2 at ambient pressure at lowest measured temperatures with the critical field B_c . Since $T^*(B)$ increases with increasing field and the magnetic susceptibility $\chi(T)$ for $B \perp c$ displays a local maximum at T^* , the crossover has been associated with a partial ferromagnetic (FM) polarization [10]. Subsequently, the crossover has been interpreted as signature of a Fermi surface reconstruction due to a Kondo breakdown for the following reasons: (i) it appears in the Hall coefficient but for $B \parallel c$ it cannot be related to an anomalous Hall effect [14] and (ii) its widths in various physical properties displays a linear temperature dependence [16]. Extrapolation to $T = 0$ therefore suggests jumps of the Hall coefficient and magnetoresistance, which were taken as evidence for a transition from small to large Fermi surface at the QCP [14–16], in agreement with the expectation for the Kondo breakdown scenario [17]. Alternatively, T^* was related to spin-flip scattering of critical quasiparticles [18] or a Zeeman-driven narrow-band Lifshitz transition [19]. The latter scenario requires, however, fine-tuning of a very narrow peak in the density of states [20].

Remarkably, $T^*(B)$ is only very weakly influenced by hydrostatic or (negative) chemical pressure, induced by partial isovalent substitutions, which enlarges or diminishes the magnetically ordered phase, leading to either $B^* < B_c$ or $B^* > B_c$, respectively [8,9]. This was ascribed to an itinerant QCP at B_c in the former and a spin-liquid regime in between B_c and B^* in the latter case [9]. However, this interpretation relies on the assumption that B^* indeed indicates a change from small to large Fermi surface volume, due to a Kondo

Published by the American Physical Society under the terms of the [Creative Commons Attribution 4.0 International](https://creativecommons.org/licenses/by/4.0/) license. Further distribution of this work must maintain attribution to the author(s) and the published article's title, journal citation, and DOI.

breakdown. In fact, it is surprising that a Kondo breakdown would be so weakly influenced by pressure or (negative) chemical pressure, which tunes the balance of the Kondo to the RKKY interaction. More recently, the Kondo breakdown interpretation of T^* was also questioned by high-resolution ARPES. At zero field and temperatures down to 1 K, it detected a large Fermi surface [21]. However, it was argued, that this temperature is still too large to observe a small Fermi surface expected within the Kondo breakdown scenario for $B < B^*$ [22] and a similar rationale was used for the absence of a significant change of scanning tunneling spectroscopy at B^* , even at 0.3 K [23]. Thus, further experimental work on the nature of T^* at $T < 0.3$ K is badly needed.

Below, we report drastic changes of T^* by partial non-isoelectronic Fe or Ni substitutions, which cannot be related to the effect of chemical pressure. A complete suppression of the crossover scale is found for 10% Fe doping and this suppression correlates with the disappearance of low-temperature FM fluctuations. Furthermore, we find for all studied single crystals that the B^* crossover widths depart from a linear T dependence and do not extrapolate to zero for $T \rightarrow 0$. Altogether, the results question whether B^* for $B \perp c$ is related to a Kondo breakdown and suggest that it results from a partial polarization of fluctuating moments [10].

Various flux-grown $\text{Yb}(\text{Rh}_{1-x}\text{T}_x)_2\text{Si}_2$ single crystals with $T = \text{Fe}$ and Ni for $x \leq 0.1$ were characterized and investigated; see the Supplemental Material (SM) [24–38]. The actual doping concentrations, which in some cases deviate from the starting compositions, have been determined with $\Delta x \sim 0.01$ precision. For low-noise alternating-current electrical resistivity and magnetic susceptibility measurements down to 20 mK, commercial low-temperature transformers were utilized in a dilution refrigerator. Measurements at enhanced temperatures were conducted in the physical property measurement system (PPMS) and magnetic property measurement system (MPMS). All experiments were carried out for $B \perp c$. For hydrostatic pressure experiments up to 1.5 GPa, a piston cylinder pressure cell with daphne oil as pressure medium has been utilized. The pressure has been determined with a superconducting lead manometer.

In the following, we discuss the influence of different non-isoelectronic substitutions on the low-temperature properties of $\text{Yb}(\text{Rh}_{1-x}\text{T}_x)_2\text{Si}_2$ in comparison with previous results of isoelectronic substitution ($T = \text{Co}$ and Ir) [9] as well as hydrostatic pressure [8]. Considering the periodic table, Ni or Fe doping enhances or reduces the number of conduction electrons in YbRh_2Si_2 , respectively. Additionally, these substitutions also induce chemical pressure and enhance the residual resistivity ρ_0 , e.g., to 1.8 and $7.6 \mu\Omega\text{cm}$ for 3 and 7.5% Fe doping, respectively, which is similar to that for respective Co substitution Ref. [24]. For undoped YbRh_2Si_2 an enhancement of ρ_0 from 0.5 to $3 \mu\Omega\text{cm}$ does not change T_N , B_c , or T^* [6,39]. Furthermore, the hydrostatic pressure dependence of these properties for undoped YbRh_2Si_2 perfectly matches with the effect of chemical pressure in $\text{Yb}(\text{Rh}_{1-x}\text{Co}_x)_2\text{Si}_2$ single crystals, for which latter the residual resistivity is enhanced, e.g., to $10.7 \mu\Omega\text{cm}$ for $x = 0.07$ [8,30]. Thus, for Fe doping the observed changes of the low-energy scales reported below are not primarily caused by the effect of disorder but rather result from chemical pressure and non-isoelectronic substitution.

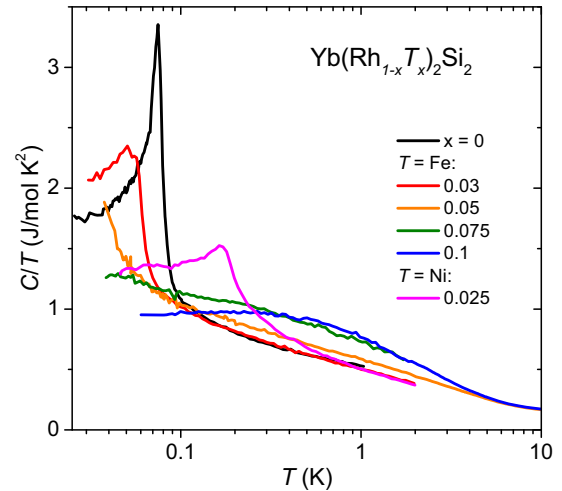


FIG. 1. Temperature dependence of the specific heat coefficient C/T (on a logarithmic scale) for various single crystals of $\text{Yb}(\text{Rh}_{1-x}\text{T}_x)_2\text{Si}_2$ ($T = \text{Fe}, \text{Ni}$) with compositions as indicated by the labels. Data for $x = 0$ were taken from [7].

Figure 1, displaying the low-temperature specific heat coefficient of various investigated single crystals, provides an overview on the tunability of the ground state by doping. The sharp peak at 75 mK for the undoped material indicates the AF phase transition [7]. Already small substitution with Fe or Ni significantly shifts the transition to lower and higher temperatures, respectively. This cannot be related to the effect of chemical pressure, which acts similarly for partial Fe, Ni, and Co substitution, as evidenced by a similar evolution of the lattice constants, resistivity maximum temperature, and Kondo temperature (see SM [24]). We therefore associate the disparate change of T_N with partial Fe and Ni substitution to non-isoelectronic substitution. For 5% Fe substitution, the steep upturn below 80 mK indicates an AF transition temperature around 40 mK, while C/T for 7.5% Fe follows a logarithmic divergence to lowest temperatures. For 10% Fe substitution, a clear saturation of C/T below 0.3 K highlights a paramagnetic Fermi liquid (FL) ground state. This evolution is unexpected, given that (i) similar chemical pressure for Co substitution enhances T_N and (ii) the isostructural end member YbFe_2Si_2 orders magnetically at 0.75 K [40]. As detailed in SM, a nonmonotonic evolution of the lattice constants and change of the CEF ground-state wave function is expected at $x(\text{Fe}) > 0.1$.

The influence of Fe or Ni substitutions on the low-temperature magnetic susceptibility is shown in Fig. 2. The AF phase transition for undoped and Ni-doped crystals results in sharp anomalies. The observed increase of the susceptibility upon cooling, following a $\chi(T) \sim T^{-0.6}$ divergence between 0.3 and 10 K (for undoped and 5% Ge-doped YbRh_2Si_2) has previously been ascribed to FM fluctuations that compete with AF fluctuations close to T_N [10,41]. Fe doping reduces the low-temperature susceptibility by a factor of 3 for $x = 0.1$ compared to undoped, 6% Ir-substituted, and 7% Co-substituted YbRh_2Si_2 [9,10]. This indicates a drastic suppression of the Sommerfeld-Wilson ratio and thus of the FM fluctuations by Fe doping.

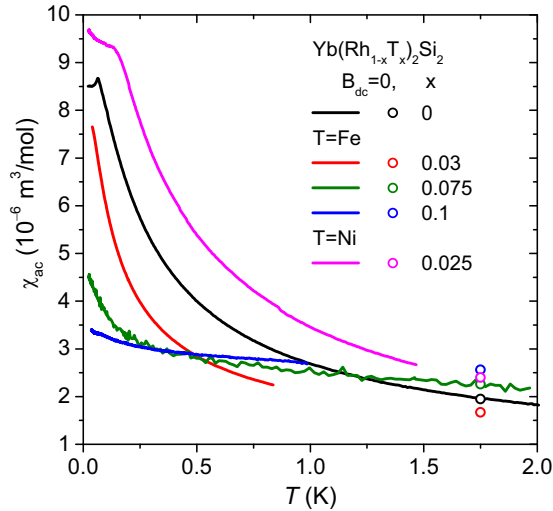


FIG. 2. Temperature dependence of the magnetic ac susceptibility (in zero dc field) for various single crystals of Yb(Rh_{1-x}T_x)₂Si₂ with compositions as indicated by the labels. All data have been taken for fields applied within the easy plane perpendicular to the *c* axis. The open circles indicate *M/B* data determined in a SQUID magnetometer (see SM [24]). Data for *x* = 0 were taken from Ref. [7].

As detailed in the Ref. [24], we fitted the magnetic susceptibility between 2 and 4 K by a Curie-Weiss law. For undoped YbRh₂Si₂, it amounts to -3 K and increases toward zero for Ni doping in a similar way as previously found for Co doping [30] (note that Co substitution tunes the ground state toward ferromagnetism [42–44]). By contrast, Fe substitution strongly enhances the negative Θ_W in accordance with a suppression of the FM fluctuations.

Next, we investigate the evolution of the $T^*(B)$ crossover with doping. To determine $T^*(B)$, we utilize $\chi(T)$ (see Ref. [24]) and the isothermal magnetoresistance. As previously done for undoped YbRh₂Si₂, the characteristic crossover field B^* is obtained by fitting of $\rho(B)$ at different temperatures to an empirical crossover function, which also allows us to determine the temperature dependence of the full width at half maximum (FWHM) of the crossover [14–16]. As shown in Fig. 3(a) for selected doped single crystals, the crossover field marks an inflection point in the negative magnetoresistance, in accordance with previous results for pure YbRh₂Si₂ [15]. While Ni doping enhances B^* , the latter is reduced by Fe doping [cf. the shift of the arrows with increasing Fe substitution in Fig. 3(a)]. In addition, also the size of the negative magnetoresistance contribution is drastically reduced. For 10% Fe substitution, the anomaly associated with B^* has completely disappeared and a featureless positive magnetoresistance behavior is found.

Figure 3(b) displays the temperature dependence of the FWHM for the various doped single crystals as determined from magnetoresistance measurements shown in Fig. 3(a). At temperatures above 0.1 K, the data agree very well with the same linear dependence (red line) found in previous magnetoresistance and Hall effect measurements up to 1 K [16]. Note that the FWHM at 0.1 K is still large, i.e., around 0.08 T, indicating that even at this low temperature, this is

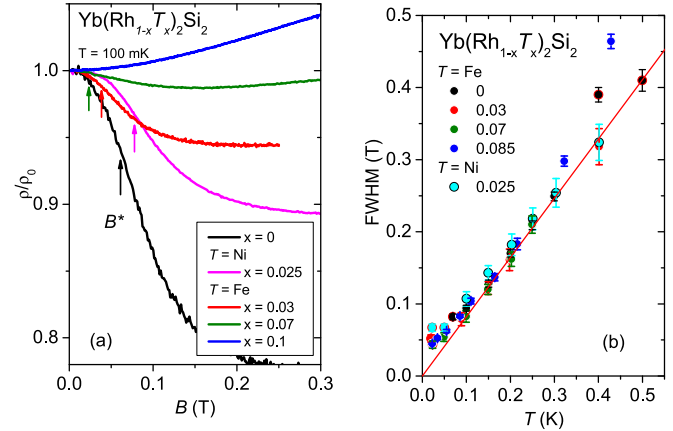


FIG. 3. Normalized isothermal magnetoresistance of various Yb(Rh_{1-x}T_x)₂Si₂ single crystals at 100 mK (a). Arrows mark B^* determined by fitting the data to an empirical crossover function of the form $f(B, T) = A_2 - (A_2 - A_1) / \{1 + [B/B^*(T)]^p\}$ [14–16]. Temperature dependence of the respective FWHM values (b). The red line indicates a linear temperature dependence and is drawn identically to that in Ref. [16].

a rather broad crossover. Clearly for all our studied systems the FWHM is above the red line below 0.1 K. Extrapolation to a zero crossover width at $T = 0$ is thus invalid. A similar trend is visible in most data sets from Ref. [16] for $x = 0$ (see Ref. [24]) and for Yb(Rh_{0.93}Co_{0.07})₂Si₂ [45], where the deviation is found at temperatures below T_N . Most important, we observe deviation from a linear T dependence also for systems in which B^* does not cross a magnetic phase boundary. One may argue that disorder introduced by chemical substitution leads to an extrinsic additional temperature-independent offset to the FWHM. However, we do not even see an increase of the FWHM with tenfold increasing residual resistivity for the systems shown in Fig. 3(b).

To disentangle the combined effect of chemical pressure and charge carrier doping on $T^*(B)$ in Yb(Rh_{1-x}Fe_x)₂Si₂, we also performed hydrostatic pressure experiments on $x = 0.07$ and $x = 0.1$ single crystals. We selected these two concentrations, because the former still shows a tiny crossover signature, while it is fully suppressed for the latter. As discussed above, for undoped YbRh₂Si₂ as well as partial isoelectronic Co and Ir substitution, the $T^*(B)$ scale is almost insensitive to pressure [8,9]. As shown in Fig. 4(a), the same holds true for the 7% Fe-doped case. The crossover field B^* at 0.2 K shifts only very weakly toward smaller values for pressures up to 0.88 GPa. On the other hand, hydrostatic pressure of this size leads to a rapid stabilization of magnetic order. This is evident from a clear dip in the temperature derivative of the electrical resistivity $d\rho/dT$ at T_N , shown in the inset of Fig. 5, which is first visible at 0.39 GPa. T_N increases with increasing pressure. Isothermal magnetoresistance measurements under hydrostatic pressure are shown in Ref. [24]. The phase diagram in Fig. 5 summarizes the anomalies from temperature (circles) and field (diamonds) sweeps. While at ambient pressure no magnetically ordered state can be detected, for a pressure of 0.39 GPa the observed Neel temperature and critical field are close to that for undoped YbRh₂Si₂ at $p = 0$. With increasing

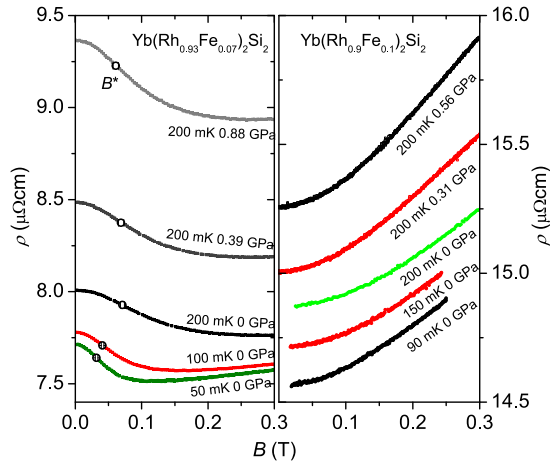


FIG. 4. Isothermal magnetoresistance of $\text{Yb}(\text{Rh}_{1-x}\text{Fe}_x)_2\text{Si}_2$ for $x = 0.07$ (a) and $x = 0.1$ (b) at various temperatures and pressures. The circles in panel (a) indicate the position of $B^*(T)$.

pressure, the AF phase boundary is enlarged while the $T^*(B)$ line does not change much. This is qualitatively similar as found previously for $\text{Yb}(\text{Rh}_{1-x}\text{Co}_x)_2\text{Si}_2$ [9] and pressurized YbRh_2Si_2 [8]. Thus, pressure is able to tune back the AF state, which has been depressed below 40 mK but only weakly changes $T^*(B)$.

Next, we discuss the pressure experiments on $\text{Yb}(\text{Rh}_{0.9}\text{Fe}_{0.1})_2\text{Si}_2$. At ambient pressure, this sample is located on the paramagnetic side of the QCP (cf. Fig. 1) and shows T^2 behavior in zero field $\rho(T)$ (see Ref. [24]), the $T^*(B)$ crossover is completely suppressed, and instead a positive magnetoresistance is found (Fig. 3). Since $x = 0.1$ is so close to $x = 0.085$ for which T^* was still observed, we were interested in whether pressure can recover the crossover for $x = 0.1$. However, even up to the maximal pressure of

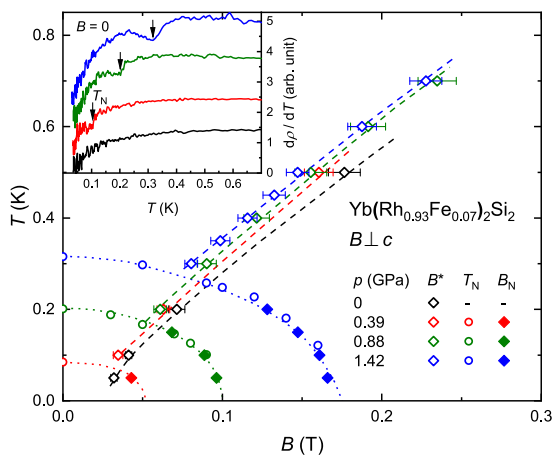


FIG. 5. Temperature field phase diagram for $\text{Yb}(\text{Rh}_{0.93}\text{Fe}_{0.07})_2\text{Si}_2$ at various hydrostatic pressures. Circles and diamonds determined from temperature and field sweeps, respectively, denote AF phase boundaries and $T^*(B)$ crossover as indicated by labels. The inset shows the signature of T_N in the temperature derivative of the electrical resistivity for different pressures. Curves are shifted upward for clarification. Arrows indicate T_N .

1.37 GPa [see SM [24] and Fig. 4(b)], magnetoresistance remains positive and the T^* crossover remains absent. Such pressure has strong influence on undoped YbRh_2Si_2 or on the $x = 0.07$ sample. Therefore, the balance between Kondo and RKKY interaction must significantly be modified by 1.37 GPa. Since this system is so close to the concentration at which the T^* crossover has been suppressed, it is therefore fully unexpected within the Kondo breakdown scenario that such significant pressure is unable to recover the change of the Fermi surface volume. Thus, these data seem incompatible with the notion that T^* indicates a Kondo breakdown. Rather than depending on pressure or chemical pressure, T^* appears to be highly sensitive to Fe or Ni doping.

Another important observation is that the size of the magnetoresistance crossover disappears before the crossover field B^* approaches zero (see SM [24]). Thus, this anomaly is a field-induced effect. The zero-field temperature-pressure/doping plane has no T^* signature, in contrast to the general expectation for local quantum criticality, where a Kondo breakdown should also occur in the absence of a magnetic field [17].

While the FM fluctuations are rather robust under positive or negative chemical pressure, Fe doping leads to a suppression of FM fluctuations (cf. Fig. 2), which coincides with the complete disappearance of the T^* crossover. This crossover thus marks a field-induced partial polarization of moments [10], indicated by an inflection point of the entropy $S(B)$ at T^* [12], which naturally explains the negative magnetoresistance. In fact, such a signature of moment polarization in susceptibility and magnetoresistance is expected in any metallic magnet by the Zeeman effect. Recently, e.g., it has been reported in NbFe_2 [46], YbNi_4P_2 [44], $\text{Ce}_3\text{Pd}_{20}\text{Si}_6$ [47], and CePdAl [48], although in the two latter cases it was interpreted as finite-temperature signature of a Kondo breakdown.

Despite the chemical pressure induced by Fe doping and the fact that pure YbFe_2Si_2 is an AF with $T_N = 0.75$ K [40], the partial substitution of Rh with Fe suppresses AF order in $\text{Yb}(\text{Rh}_{1-x}\text{Fe}_x)_2\text{Si}_2$. For $x = 0.1$, a stable Fermi liquid state develops, which lacks any T^* crossover. Isoelectronic substitution of Rh by Co or Ir corresponds to positive or negative chemical pressure and does not modify the $T^*(B)$ crossover line. On the other hand, non-isovalent Fe and Ni substitutions depress and enlarge $T^*(B)$, respectively.

The previous interpretation of $T^*(B)$ (for $B \perp c$ and $B \parallel c$) in YbRh_2Si_2 as finite-temperature signature of a Kondo breakdown is questioned by the following observations when tuning $T^*(B)$ by non-isoelectronic substitutions: (1) the crossover width does not extrapolate to zero, (2) the T^* anomaly requires a finite magnetic field, (3) in contrast to the Kondo temperature, it is almost insensitive to pressure, and (4) it coheres with FM fluctuations, i.e., once the latter are depressed, T^* disappears.

We thank M. Brando, J. Dong, S. Friedemann, C. Geibel, S. Lausberg, Q. Si, C. Stingl, M. Vojta and K. Winzer for valuable discussions. This work was supported by the German Science Foundation (DFG) research unit 960 ‘‘Quantum phase transitions.’’

- [1] B. J. Ramshaw, S. E. Sebastian, R. D. McDonald, J. Day, B. S. Tan, Z. Zhu, J. B. Betts, R. Liang, D. A. Bonn, W. N. Hardy, and N. Harrison, *Science* **348**, 317 (2015).
- [2] J. Custers, P. Gegenwart, H. Wilhelm, K. Neumaier, Y. Tokiwa, O. Trovarelli, C. Geibel, F. Steglich, C. Pépin, and P. Coleman, *Nature (London)* **424**, 524 (2003).
- [3] H. v. Löhneysen, A. Rosch, M. Vojta, and P. Wölfle, *Rev. Mod. Phys.* **79**, 1015 (2007).
- [4] P. Gegenwart, Q. Si, and F. Steglich, *Nat. Phys.* **4**, 186 (2008).
- [5] N. D. Mathur, F. M. Grosche, S. R. Julian, I. R. Walker, D. M. Freye, R. K. W. Haselwimmer, and G. G. Lonzarich, *Nature (London)* **394**, 39 (1998).
- [6] O. Trovarelli, C. Geibel, S. Mederle, C. Langhammer, F. M. Grosche, P. Gegenwart, M. Lang, G. Sparn, and F. Steglich, *Phys. Rev. Lett.* **85**, 626 (2000).
- [7] P. Gegenwart, J. Custers, C. Geibel, K. Neumaier, T. Tayama, K. Tenya, O. Trovarelli, and F. Steglich, *Phys. Rev. Lett.* **89**, 056402 (2002).
- [8] Y. Tokiwa, P. Gegenwart, C. Geibel, and F. Steglich, *J. Phys. Soc. Jpn.* **78**, 123708 (2009).
- [9] S. Friedemann, T. Westerkamp, M. Brando, N. Oeschler, S. Wirth, P. Gegenwart, C. Krellner, C. Geibel, and F. Steglich, *Nat. Phys.* **5**, 465 (2009).
- [10] P. Gegenwart, J. Custers, Y. Tokiwa, C. Geibel, and F. Steglich, *Phys. Rev. Lett.* **94**, 076402 (2005).
- [11] R. Küchler, N. Oeschler, P. Gegenwart, T. Cichorek, K. Neumaier, O. Tegus, C. Geibel, J. A. Mydosh, F. Steglich, L. Zhu, and Q. Si, *Phys. Rev. Lett.* **91**, 066405 (2003).
- [12] Y. Tokiwa, T. Radu, C. Geibel, F. Steglich, and P. Gegenwart, *Phys. Rev. Lett.* **102**, 066401 (2009).
- [13] A. J. Millis, *Phys. Rev. B* **48**, 7183 (1993).
- [14] S. Paschen, T. Lühmann, S. Wirth, P. Gegenwart, O. Trovarelli, C. Geibel, F. Steglich, P. Coleman, and Q. Si, *Nature (London)* **432**, 881 (2004).
- [15] P. Gegenwart, T. Westerkamp, C. Krellner, Y. Tokiwa, S. Paschen, C. Geibel, F. Steglich, E. Abrahams, and Q. Si, *Science* **315**, 969 (2007).
- [16] S. Friedemann, N. Oeschler, S. Wirth, C. Krellner, C. Geibel, F. Steglich, S. Paschen, S. Kirchner, and Q. Si, *Proc. Natl. Acad. Sci. USA* **107**, 14547 (2010).
- [17] Q. Si, S. Rabello, K. Ingersent, and J. L. Smith, *Nature (London)* **413**, 804 (2001).
- [18] P. Wölfle and E. Abrahams, *Phys. Rev. B* **92**, 155111 (2015).
- [19] A. Hackl and M. Vojta, *Phys. Rev. Lett.* **106**, 137002 (2011).
- [20] S. Friedemann, S. Paschen, C. Geibel, S. Wirth, F. Steglich, S. Kirchner, E. Abrahams, and Q. Si, *Phys. Rev. Lett.* **111**, 139701 (2013).
- [21] K. Kummer, S. Patil, A. Chikina, M. Güttler, M. Höppner, A. Generalov, S. Danzenbächer, S. Seiro, A. Hannaske, C. Krellner *et al.*, *Phys. Rev. X* **5**, 011028 (2015).
- [22] S. Paschen, S. Friedemann, S. Wirth, F. Steglich, S. Kirchner, and Q. Si, *J. Magn. Magn. Mater.* **400**, 17 (2016).
- [23] S. Seiro, L. Jiao, S. Kirchner, S. Hartmann, S. Friedemann, C. Krellner, C. Geibel, Q. Si, F. Steglich, and S. Wirth, *Nat. Commun.* **9**, 3324 (2018).
- [24] See Supplemental Material at <http://link.aps.org/supplemental/10.1103/PhysRevResearch.1.032004> for further information on single-crystal growth and characterization, electrical resistivity, heat capacity and magnetic susceptibility, magnetoresistance, electrical resistivity measurements under hydrostatic pressure, the T^* crossover for fields parallel to the c axis, and the temperature dependence of the FWHM [25–38].
- [25] M. Mchalwat, Master's thesis, Universität Göttingen, Göttingen, Germany, 2011 (unpublished).
- [26] E. Blumenröther, Master's thesis, Universität Göttingen, Göttingen, Germany, 2013 (unpublished).
- [27] M. Schubert, Ph.D. dissertation, Universität Göttingen, Göttingen, Germany, 2014 (unpublished).
- [28] C. Krellner, Ph.D. dissertation, TU Dresden, Dresden, Germany, 2009 (unpublished).
- [29] C. Krellner, S. Taube, T. Westerkamp, Z. Hossain, and C. Geibel, *Philos. Mag.* **92**, 2508 (2012).
- [30] C. Klingner, C. Krellner, M. Brando, C. Geibel, F. Steglich, D. V. Vyalikh, K. Kummer, S. Danzenbächer, S. L. Molodtsov, C. Laubschat *et al.*, *Phys. Rev. B* **83**, 144405 (2011).
- [31] D. Rossi, R. Marazza, and R. Ferro, *J. Less Common Met.* **58**, 203 (1978).
- [32] D. R. Noakes, A. M. Umarji, and G. K. Shenoy, *J. Magn. Magn. Mater* **39**, 309 (1983).
- [33] J. J. Bara, H. U. Hryniewicz, A. Milos, and A. Szytula, *J. Less Common Met.* **161**, 185 (1990).
- [34] T. Mori, S. Kitayama, Y. Kanai, S. Naimen, H. Fujiwara, A. Higashiya, K. Tamasaku, A. Tanaka, K. Terashima, S. Imada *et al.*, *J. Phys. Soc. Jpn.* **83**, 123702 (2014).
- [35] S. Mederle, R. Borth, C. Geibel, F. M. Grosche, G. Sparn, O. Trovarelli, and F. Steglich, *J. Phys.: Condens. Matter* **14**, 10731 (2002).
- [36] J. Sichelschmidt, H. S. Jeevan, M. Mchalwat, and P. Gegenwart, *Phys. Stat. Sol.* **250**, 495 (2013).
- [37] S.-H. Hübner, Master's thesis, Universität Göttingen, Göttingen, Germany, 2014 (unpublished).
- [38] S. Friedemann, Ph.D. dissertation, TU Dresden, Dresden, Germany, 2009 (unpublished).
- [39] C. Krellner, S. Hartmann, A. Pikul, N. Oeschler, J. G. Donath, C. Geibel, F. Steglich, and J. Wosnitza, *Phys. Rev. Lett.* **102**, 196402 (2009).
- [40] J. A. Hodges, *Europhys. Lett.* **4**, 749 (1987).
- [41] P. Gegenwart, Y. Tokiwa, J. Custers, C. Geibel, and F. Steglich, *J. Phys. Soc. Jpn.* **75**, 155 (2006).
- [42] S. Lausberg, A. Hannaske, A. Steppke, L. Steinke, T. Gruner, L. Pedrero, C. Krellner, C. Klingner, M. Brando, C. Geibel *et al.*, *Phys. Rev. Lett.* **110**, 256402 (2013).
- [43] S. Hamann, J. Zhang, D. Jang, A. Hannaske, L. Steinke, S. Lausberg, L. Pedrero, C. Klingner, M. Baenitz, F. Steglich *et al.*, *Phys. Rev. Lett.* **122**, 077202 (2019).
- [44] S. Lausberg, Ph.D. dissertation, TU Dresden, Dresden, Germany, 2013 (unpublished).
- [45] M. Brando, L. Pedrero, T. Westerkamp, C. Krellner, P. Gegenwart, C. Geibel, and F. Steglich, *Phys. Stat. Solidi B* **250**, 485 (2013).
- [46] D. Rauch, Ph.D. dissertation, TU Braunschweig, Braunschweig, Germany, 2015 (unpublished).
- [47] J. Custers, K.-A. Lorenzer, M. Müller, A. Prokofiev, A. Sidorenko, H. Winkler, A. M. Strydom, Y. Shimura, T. Sakakibara, R. Yu *et al.*, *Nat. Mater.* **11**, 189 (2012).
- [48] J. Zhang, H. Zhao, M. Lv, S. Hu, Y. Isikawa, Y.-f. Yang, Q. Si, F. Steglich, and P. Sun, *Phys. Rev. B* **97**, 235117 (2018).